Measuring orientation of human body segments using miniature gyroscopes and accelerometers

H. J. Luinge   P. H. Veltink

Signals Systems Group, Department of Electrical Engineering, University of Twente,
Enschede, The Netherlands

Abstract—*In the medical field, there is a need for small ambulatory sensor systems for measuring the kinematics of body segments. Current methods for ambulatory measurement of body orientation have limited accuracy when the body moves. The aim of the paper was to develop and validate a method for accurate measurement of the orientation of human body segments using an inertial measurement unit (IMU). An IMU containing three single-axis accelerometers and three single-axis micromachined gyroscopes was assembled in a rectangular box, sized $20 \times 20 \times 30$ mm. The presented orientation estimation algorithm continuously corrected orientation estimates obtained by mathematical integration of the 3D angular velocity measured using the gyroscopes. The correction was performed using an inclination estimate continuously obtained using the signal of the 3D accelerometer. This reduces the integration drift that originates from errors in the angular velocity signal. In addition, the gyroscope offset was continuously recalibrated. The method was realised using a Kalman filter that took into account the spectra of the signals involved as well as a fluctuating gyroscope offset. The method was tested for movements of the pelvis, trunk and forearm. Although the problem of integration drift around the global vertical continuously increased in the order of $0.5° \ s^{-1}$, the inclination estimate was accurate within $3°$ RMS. It was shown that the gyroscope offset could be estimated continuously during a trial. Using an initial offset error of $1 \ rad \ s^{-1}$, after 2 min the offset error was roughly 5% of the original offset error. Using the Kalman filter described, an accurate and robust system for ambulatory motion recording can be realised.*

Keywords—*Gyroscope, Accelerometer, Kalman, Human, Kinematics*

1 Introduction

SINCE MICROMACHINED sensors such as gyroscopes and accelerometers have become generally available, human movement can be measured continuously outside a specialised laboratory with ambulatory systems. Applications involve monitoring activities of daily living (ADL) and level of activity (BOUTEN, et al., 1997; FOERSTER et al., 1999; USWATTE, 2000; VELTINK et al., 1996; MATHIE et al., 2003), gait analysis (TONG and GRANAT, 1999; WILLIAMSON and ANDREWS, 2001; MAYAGOITIA et al., 2002; WILLEMSEN et al., 1990b; MIYAZAKI, 1997; MOE-NILSSEN, 1998; MOE-NILSSEN and HELBOSTAD, 2004; PAPPAS et al., 2001), research into motor control and stability (DINGWELL et al., 2000; ALUSI et al., 2001; NAJAFI et al., 2002; MANSON et al., 2000), load estimation (BATEN et al., 1996; VAN DEN BOGERT et al., 1996) or functional electrical stimulation (WILLEMSEN et al., 1990a; WILLIAMSON and

ANDREWS, 2000; SWEENEY et al., 2000; TONG and GRANAT, 1998; VELTINK et al., 2003).

In many of these applications, orientation is an essential quantity to be estimated. If accelerometers and gyroscopes are to be used for load estimation using inverse dynamics techniques, the orientation and angular velocity, as well as the acceleration, of a segment have to be known. Also, the identification of daily tasks will be more detailed once the orientation can be measured. Acceleration can be used to analyse stability. Measurement of acceleration with a body-mounted accelerometer will be more accurate once the inclination with respect to gravity is known.

A 3D accelerometer unit can be used as an inclinometer in the absence of acceleration (KEMP et al., 1998; LÖTTERS et al., 1998; WILLEMSEN et al., 1990b; BERNMARK and WIKTORIN, 2002; HANSSON et al., 2001). Under this condition, it measures the angle of the sensor unit with respect to gravity. This method is appropriate if the magnitude of the acceleration can be neglected with respect to the gravity, but will be less accurate for movements with relatively large accelerations. Furthermore, accelerometer signals do not contain information about the rotation around the vertical and therefore do not give a complete description of orientation. The accuracy of an inclination estimate can be increased using a Kalman filter and

a model of the spectrum of the acceleration (LUINGE and VELTINK, 2004). It was suggested that, to increase accuracy, gyroscopes could be used in addition to accelerometers.

A gyroscope measures angular velocity. Change in orientation can be estimated by integrating the angular velocity according to an algorithm such as given by Bortz or Ignagni (BORTZ, 1971; IGNAGNI, 1990). However, an error in measured angular velocity will result in increasing inaccuracy in the estimated orientation. In particular, a relatively small offset on the gyroscope signal will give rise to large integration errors, restricting the time of accurate measurement to less than 1 min for current commercially available micromachined gyroscopes. Moreover, if an absolute orientation is required instead of a change in orientation, a reference orientation has to be obtained at least once during a recording.

Orientation can be estimated by combining the sensor signals from gyroscopes and accelerometers. This has already been performed in the automotive field (BARSHAN and DURRANT-WHYTE, 1995) and for the assessment of human balancing (BASELLI et al., 2001). The design of a filter for estimation of the orientation of human body segments has been described by BACHMAN (2000) and FOXLIN (1996). Bachman used a filter that relied on accelerometers and magnetometers for low-frequency components of the orientation and used gyroscopes to measure faster changes of orientation. This method seemed to be robust, although the performance of the filter has not been investigated for 3D human movements. It did not take the different error sources explicitly into account. In particular, the use of magnetometers could give large errors in the vicinity of ferromagnetic materials. Foxlin described a sensor unit containing a 2D fluid inclinometer, a 2D electronic compass and 3D gyroscopes, with a Kalman filter that incorporated a continuous gyroscope offset estimate. Although this method seemed to work for some controlled 2D test movements, applicability of this sensor was limited for general 3D movements, owing to the singularities arising from the 2D instead of 3D sensors and the use of Euler angles.

The aim of this paper was to design and evaluate a Kalman filter that fuses triaxial accelerometer and triaxial gyroscope signals for ambulatory recording of human body segment orientation. It obtains the orientation in a statistical, most-likely sense, given clear assumptions about the movement that is to be recorded and about the sensor error behaviour. Because of this, it can be assumed that the solution is the best given the assumptions that can be made. The Kalman states that are continuously corrected include the orientation and offset errors. Body segment orientation obtained with this 3D inertial measurement unit was compared with an orientation obtained using a laboratory bound camera system. The movement of pelvis and trunk during lifting tasks and the forearm movement during some ADL tasks were recorded.

2 Design of an optimum filter for orientation estimation

2.1 Sensor fusion with a Kalman filter

A complementary Kalman filter (KALMAN, 1960; BROWN and HWANG, 1997) was designed to estimate orientation by combining the three accelerometer and three gyroscope signals using a model of the inertial measurement unit (IMU) system and relevant signals. The structure of the estimation procedure is shown in Fig. 1. Based on a model describing the sensor signals, both the 3D gyroscope and 3D accelerometer systems yield a measure of inclination ($\hat{Z}_G^-$ and $\hat{Z}_A^-$, respectively), each with different accuracies and error sources. The inclination difference ($\hat{Z}_A^- - \hat{Z}_G^-$) is a function of errors in the two measurement systems, particularly an
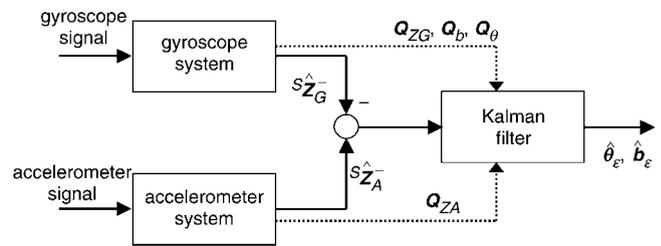

Fig. 1 *Structure of Kalman filter estimation. Both accelerometer and gyroscope system are used to make estimate of global vertical unit vector($^S\hat{Z}_A$ and $^S\hat{Z}_G$, respectively) and system error covariances. Covariances are Q_b for offset uncertainty, Q_θ for orientation uncertainty and Q_{ZG} and Q_{ZA} for vertical uncertainty. Difference between two inclination estimates $^S\hat{Z}_A - ^S\hat{Z}_G$ is written as function of orientation and offset errors. Kalman filter uses function with covariances and inclination difference to estimate these orientation and offset errors ($\hat{\theta}_\varepsilon$ and $\hat{b}_\varepsilon$, respectively)*

orientation error and a gyroscope offset error in the gyroscope system. This function is also known as the error model. The Kalman filter uses the inclination difference with the error model to estimate the orientation and offset errors in a statistical, most-likely manner. These orientation errors and offset errors are then used to correct the orientation and offset at each timestep.

To implement the Kalman filter requires an error model in state space format that gives the inclination difference as a function of orientation errors, offset errors and measurement noise. This error model was derived by first describing a model of the sensor output and considering the effect of uncertain model states on the inclination estimate. The model of the sensor output is based on only a few clear assumptions regarding the sensor system and the movement that is to be recorded, so that any tuning of the parameters of the Kalman filter has a clear interpretation, and the orientation estimate is optimum within the given assumptions.

2.2 Model of sensor signals

The sensor is assumed to be attached to a human body segment that rotates and translates with respect to a global co-ordinate frame. A model of the measured signals is based on the following assumptions (Fig. 2):
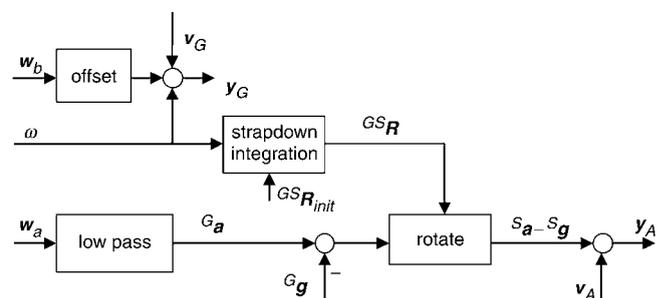

Fig. 2 *Sensor signal model. Model of relationships between segment kinematics and measured gyroscope and accelerometer signals (y_G and y_A). Gyroscope signal is modelled as slowly varying offset plus angular velocity ω and white measurement noise v_G. Relationship between angular velocity and orientation ^{GS}R is described in box labelled 'strapdown integration'. Accelerometer signal is composed of acceleration and gravity contribution, expressed in sensor frame (^Sa-^Sg) plus measurement noise vector v_A. Acceleration of segment is modelled as low-pass filtered white noise, and gravity is constant vector*

(a) a gyroscope measures a 3D angular velocity plus an offset and white measurement noise in the sensor co-ordinate frame

(b) the spectrum of the gyroscope offset has a low cutoff frequency in comparison with the bandwidth of the kinematic signals that are to be measured

(c) a 3D accelerometer measures acceleration minus gravity and a white noise component, all in the sensor co-ordinate frame

(d) the acceleration of a body segment in the global system can be described as low pass filtered white noise.

Using assumption (a), the signals as measured using the gyroscope system (described by the column vector $\mathbf{y}_G = [y_{G,x}\ y_{G,y}\ y_{G,z}]^T$) are assumed to be the sum of the angular velocity vector $\boldsymbol{\omega}_t$, a slowly varying offset vector ($\boldsymbol{b}_t$) and a three-element white Gaussian noise vector $\mathbf{v}_{G,t}$. The variation of the offset is assumed to be caused by slowly changing properties of the sensor, e.g. mechanical wear and temperature sensitivity.

$$\mathbf{y}_{G,t} = \boldsymbol{\omega}_t + \boldsymbol{b}_t + \mathbf{v}_{G,t} \tag{1}$$

The slow variation of the gyroscope offset $\boldsymbol{b}$ is modelled as a realisation of a first-order Markov process, driven by a small white Gaussian noise vector $\boldsymbol{w}_{b,t}$

$$\boldsymbol{b}_t = \boldsymbol{b}_{t-1} + \boldsymbol{w}_{b,t} \tag{2}$$

The three accelerometer signals are modelled as the sum of the linear acceleration vector ($\boldsymbol{a}_t$), the gravity vector $\boldsymbol{g}$ and a white Gaussian noise signal $\mathbf{v}_A$.

$$\mathbf{y}_{A,t} = {}^S\boldsymbol{a}_t - {}^S\boldsymbol{g}_t + \mathbf{v}_{A,t} \tag{3}$$

In (3), a superscript S is used to indicate vectors that are expressed in the sensor co-ordinate system.

The acceleration was modelled as a first order low-pass filtered white noise process according to

$${}^G\boldsymbol{a}_t = c_a \cdot {}^G\boldsymbol{a}_{t-1} + \boldsymbol{w}_{a,t} \tag{4}$$

where c_a is a dimensionless constant that determines the cutoff frequency. The superscript G is used to denote a vector that is expressed in the global co-ordinate system.

A strapdown integration algorithm calculates the change in orientation from an angular velocity signal. The word strapdown means that the angular velocity is obtained using gyroscopes strapped to an object. A number of integration methods have been described (IGNAGNI, 1990; BORTZ, 1971; JIANG and LIN, 1992). The orientation of the sensor with respect to the global co-ordinate frame is expressed with a rotation matrix, containing the three unit column vectors of the global co-ordinate system expressed in the sensor co-ordinate system (5).

$${}^{GS}\boldsymbol{R} = \begin{bmatrix} {}^S\boldsymbol{X} & {}^S\boldsymbol{Y} & {}^S\boldsymbol{Z} \end{bmatrix}^T \tag{5}$$

The acceleration and gravity in the global co-ordinate frame (4) are related to the acceleration and gravity in the sensor co-ordinate frame (3) through the axes transformation of (6).

$${}^G\boldsymbol{a}_t - {}^G\boldsymbol{g}_t = {}^{GS}\boldsymbol{R}_t \cdot \left({}^S\boldsymbol{a}_t - {}^S\boldsymbol{g}_t \right) \tag{6}$$

2.3 Inclination estimation based on sensor model

The sensor model was used to make two estimates of the inclination, one on the basis of the 3D gyroscope signals and one on the basis of the accelerometer signals. Fig. 3 describes the estimation procedure. The inclination was defined as the estimate of the vertical direction by the IMU. Because the global Z-axis was defined in the vertical direction, the inclination was expressed as ${}^S\boldsymbol{Z}_t$, the Z-axis of the global co-ordinate system expressed in the sensor co-ordinate frame.

The offset, angular velocity and acceleration are estimated using (2), (1), (3) and (4) and setting unknown white noise components $\boldsymbol{w}_{b,t}$, $\mathbf{v}_{G,t}$, $\mathbf{v}_{A,t}$ and $\boldsymbol{w}_{a,t}$ to zero. The estimated angular velocity $\hat{\boldsymbol{\omega}}_t^-$ and the estimated orientation at the previous timestep ${}^{GS}\hat{\boldsymbol{R}}_{t-1}^+$ are then used to calculate the current orientation according to the algorithm proposed by IGNAGNI (1990). The third row of the resulting rotation matrix (5) gives the inclination based upon the gyroscope signals ${}^S\hat{\boldsymbol{Z}}_{g,t}^-$.

A hat on top of a symbol denotes an estimate, a minus superscript denotes the a priori estimate that is made using the sensor model, and a plus superscript denotes an estimate that is made after correction by the Kalman filter.

The inclination estimated from the accelerometer is achieved by subtracting the predicted acceleration $\hat{\boldsymbol{a}}_t^-$ from the accelerometer signal to obtain the gravity vector. The gravity estimate is normalised and reversed to produce an estimation of the inclination ${}^S\hat{\boldsymbol{Z}}_{A,t}^-$.

$${}^S\hat{\boldsymbol{Z}}_A^- = \frac{\mathbf{y}_t - {}^S\hat{\boldsymbol{a}}_t^-}{\left| \mathbf{y}_t - {}^S\hat{\boldsymbol{a}}_t^- \right|} \tag{7}$$

2.4 Error model

A Kalman filter uses a state space representation to model the relationship between errors in estimated model variables x_ε and the error in the inclination predicted by the model (8).

$$\begin{aligned} \boldsymbol{x}_{\varepsilon,t} &= \boldsymbol{A} \cdot \boldsymbol{x}_{\varepsilon,t-1} + \boldsymbol{w}_t \\ \boldsymbol{z}_{\varepsilon,t} &= \boldsymbol{C} \cdot \boldsymbol{x}_{\varepsilon,t} + \boldsymbol{v}_t \end{aligned} \tag{8}$$

where $\boldsymbol{w}_t$ and $\boldsymbol{v}_t$ are Gaussian white noise processes specified by covariance matrices $\boldsymbol{Q}_{w,t}$ and $\boldsymbol{Q}_{v,t}$, respectively. The measurement difference vector $\boldsymbol{z}_\varepsilon$ is formed by the
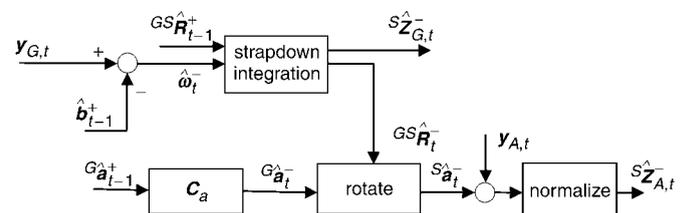

Fig. 3 *Diagram describing estimation of inclination of human body segment based on gyroscope system and based on accelerometer system using sensor signals, previously estimated states and model described in Fig. 2. Angular velocity $\boldsymbol{\omega}_t$ is estimated by subtracting estimated offset from gyroscope signal y_t. Strapdown integration algorithm is used to estimate change in orientation ${}^{GS}\hat{\boldsymbol{R}}_t$ and inclination ${}^S\hat{\boldsymbol{Z}}_{G,t}$. Acceleration ${}^G\hat{\boldsymbol{a}}_t$ is estimated by assuming it is factor c_a of previously measured acceleration. Orientation is used to estimate acceleration in sensor co-ordinate system, enabling measurement of inclination based on accelerometers ${}^S\hat{\boldsymbol{Z}}_{A,t}$*

difference between the gyroscope and accelerometer inclination estimates.

$$z_{\varepsilon,t} = {}^S\hat{Z}_A - {}^S\hat{Z}_G \qquad (9)$$

A difference in the two inclination estimates is caused by prediction errors. The two most important factors causing an inclination error are incorporated in the error state vector x_ε, which is estimated using the Kalman filter (10). The first factor is the orientation error at the previous timestep, as this orientation is used as a starting point to obtain the next orientation by strapdown integration. The second factor is the gyroscope offset error, as, already, a small offset error causes a dramatic effect on the estimated orientation.

$$x_{\varepsilon,t} = \begin{bmatrix} \theta_{\varepsilon,t-1} & b_{\varepsilon,t} \end{bmatrix}^T \qquad (10)$$

The orientation error is defined as the angle and direction is which the actual sensor co-ordinate frame has to be rotated to coincide with the estimated sensor co-ordinate frame. It is expressed by θ_ε, which has a magnitude that equals the angle of rotation, whereas the rotation axis is given by the direction of θ_ε. As other error sources are not incorporated into the state vector, these are only specified as part of the covariance matrix of w_t and v_t.

To use the Kalman filter to make an estimate of the error vector x_ε, the matrices A and C and the covariance matrices Q_w and Q_v are derived. Matrix A and noise w describe the propagation of the a priori error state vector x_ε. They were found by considering the effect of unknown system components on the error state. Matrix C and noise v describe the relationship between the error states and the Kalman filter input z_ε. They were found by considering the effect of an offset and orientation error on the inclination estimate. The covariances Q_v and Q_w were derived by taking the variances of v and w.

2.4.1 Error propagation

The offset prediction error is denoted by $\hat{b}_{\varepsilon,t-1}^-$ and can be found by substituting the prediction of the offset in the offset model (2).

$$\begin{aligned} b_{\varepsilon,t}^- &= \hat{b}_t^- - b_t \\ &= b_{\varepsilon,t-1}^+ - w_{b,t} \end{aligned} \qquad (11)$$

For small errors, the relationship between the actual and estimated orientations is given by (12) (BORTZ, 1971)

$$^{GS}\hat{R} = {}^{GS}R \cdot (I + [\theta_\varepsilon \times]) \qquad (12)$$

The matrix cross product operator is given by

$$[a\times] = \begin{bmatrix} 0 & -a_z & a_y \\ a_z & 0 & -a_x \\ -a_y & a_x & 0 \end{bmatrix}$$

The orientation after one integration step is found by considering a first order approximation of a strapdown integration step

$$^{GS}\hat{R}_t^- = {}^{GS}\hat{R}_{t-1}^+ + {}^{GS}\hat{R}_{t-1}^+ \cdot \left[T\hat{\omega}_t^- \times \right] \qquad (13)$$

where T is the sample time. An expression for the angular velocity estimate $\hat{\omega}_t^-$ was found by substituting the gyroscope

output (1) and the expression for the offset error (11) into the definition of the angular velocity error

$$\begin{aligned} \hat{\omega}_{\varepsilon,t}^- &= \hat{\omega}_t^- - \omega_t \\ &= w_{b,t} - b_{\varepsilon,t-1}^+ + v_{G,t} \end{aligned} \qquad (14)$$

If we substitute the angular velocity estimation and the orientation estimation (13) and neglect products of errors, the estimated orientation is given by

$$^{GS}\hat{R}_t^- \approx {}^{GS}R_t \cdot (I + [(\theta_{\varepsilon,t-1}^+ - Tb_{\varepsilon,t-1}^+ + Tv_{G,t})\times]) \qquad (15)$$

Finally, comparing (15) with (12), it follows that the error propagation $\theta_{\varepsilon,t}$ is described by

$$\theta_{\varepsilon,t}^- = \theta_{\varepsilon,t-1}^+ - Tb_{\varepsilon,t-1}^+ + Tv_{G,t} \qquad (16)$$

The matrix A of (8) describes the propagation of the a priori error state vector x_ε. Considering (16) and (11), it can be found that the a priori expected errors $b_{\varepsilon,t}^-$ and $\theta_{\varepsilon,t}^-$ do not depend on previous a priori estimated states $b_{\varepsilon,t-1}^-$ and $\theta_{\varepsilon,t-1}^-$. This means that knowledge about previous errors is incorporated into the current estimate, and that there is no correlation left between the a priori estimate errors of two timesteps. Therefore the A matrix equals the zero matrix.

2.4.2 Relationship between filter input and error states

The error of the gyroscope based inclination estimate was obtained in the same way as the error in the orientation estimate (15), yielding

$$\begin{aligned} {}^S\hat{Z}_{G,t}^- &\approx Z_t + {}^S\hat{Z}_{t-1} \times \theta_{\varepsilon,t-1}^+ - T{}^S\hat{Z}_{t-1} \times b_{\varepsilon,t} \\ &\quad + T{}^S\hat{Z}_{t-1} \times v_{G,t} \end{aligned} \qquad (17)$$

The error of the accelerometer-based inclination estimate ${}^S\hat{Z}_A$, (7) depends on the error in estimated acceleration expressed in the sensor co-ordinate frame and the accelerometer noise. The error in predicted acceleration in the global co-ordinate frame was found by comparing the real acceleration with the estimate, using (4).

$$\begin{aligned} {}^G a_{\varepsilon,t}^- &= {}^G\hat{a}_t^- - {}^G a_t \\ &= c_a \cdot {}^G\hat{a}_{\varepsilon,t-1}^+ - w_{a,t} \end{aligned} \qquad (18)$$

To obtain the acceleration error in the sensor co-ordinate frame, relationship (6) was applied using the acceleration error estimate (18) and orientation estimate (12). The resulting error is caused by both an orientation error and an error in the global acceleration estimate (19).

$$\begin{aligned} {}^S a_{\varepsilon,t} &= {}^S\hat{a}_t^- - {}^S a_t \\ &= c_a \cdot {}^S a_{\varepsilon,t-1} - {}^S w_{a,t} + {}^S\hat{a}_t^- \times \theta_{\varepsilon,t} \end{aligned} \qquad (19)$$

Then the accelerometer-based inclination estimate can be found using (7), where y is given by (3)

$$^S\hat{Z}_{A,t}^- = Z_t + \frac{1}{g}\left(-{}^S\hat{a}_t^- \times \theta_{\varepsilon,t} - c_a \cdot {}^S a_{\varepsilon,t} + {}^S w_{a,t} + v_{A,t} \right) \qquad (20)$$

In (20), the magnitude of the accelerometer output vector is approximated by the gravitational constant g, and products of errors are neglected.

The relationship between the inclination difference and the filter states (8) was found by substitution of (17) and (20) into (9) and use of the matrix format of the cross product to obtain the relationship as a matrix multiplication.

$$z_{\varepsilon,t} = {}^S\hat{Z}_A - {}^S\hat{Z}_G$$

$$= \left({}^S\hat{Z}_{t-1} - \frac{{}^S\hat{a}_t^-}{g}\right) \times \theta_{\varepsilon,t} + T^S\hat{Z}_{t-1} \times b_{\varepsilon,t}$$

$$+ \frac{1}{g}\left({}^S w_{a,t} - c_a \cdot {}^S a_{\varepsilon,t} + v_{A,t}\right) - {}^S\hat{Z}_{t-1} \times T \cdot v_{G,t}$$

$$= C \cdot \left\{\begin{matrix} \theta_{\varepsilon,t} \\ b_{\varepsilon,t} \end{matrix}\right\} + v_t \qquad (21)$$

where C is a 3×6 matrix, consisting of two 3×3 cross product matrices.

$$C = \left\{\left[\left(\hat{Z}_t - \frac{{}^S\hat{a}_t^-}{g}\right)\times\right] \quad \left[T \cdot \hat{Z}_t \times\right]\right\} \qquad (22)$$

The noise term v_t is described by the third and fourth terms of (21)

$$v_t = \frac{1}{g}\left({}^S w_{a,t} - c_a \cdot {}^S a_{\varepsilon,t} + +v_{A,t}\right) - {}^S Z_{t-1} \times v_{G,t} \qquad (23)$$

2.4.3 Covariance matrices

The error covariance matrix $Q_{w,t}$ of the noise term w in the error propagation part of the Kalman filter (8) can be obtained using the knowledge that the matrix A equals the zero matrix. Therefore the error covariance matrix can be found by taking the variance of the error propagation equations (11) and (16).

$$Q_{w,t} = \begin{bmatrix} E(\theta_{\varepsilon,t}^- \cdot \theta_{\varepsilon,t}^{-T}) & E(\theta_{\varepsilon,t}^- \cdot b_{\varepsilon,t}^T) \\ E(b_{\varepsilon,t}^- \cdot \theta_{\varepsilon,t}^{-T}) & E(b_{\varepsilon,t}^- \cdot b_{\varepsilon,t}^{-T}) \end{bmatrix}$$

$$= \begin{bmatrix} Q_{\theta,t-1}^+ + T^2 Q_{b,t-1}^+ + T^2 Q_{vG} & T^2 Q_{b,t-1}^+ \\ T^2 Q_{b,t-1}^+ & Q_{b,t-1}^+ + Q_b \end{bmatrix}$$

where $Q_{\theta,t-1}^+$ and $\mathbf{Q}_{b,t-1}^+$ are the *a posteriori* error covariance matrices of the orientation and offset at the previous timestep, respectively. Q_b is the very small covariance matrix of the offset noise w_b and Q_{vG} is the gyroscope noise covariance matrix.

Taking the covariance of the noise term (23) yields

$$Q_{v,t} = \frac{1}{g^2}\left(c_a^2 \cdot Q_{a,t-1}^+ + Q_{wa} + Q_{va}\right) + Q_{vG} \qquad (24)$$

where $Q_{a,t-1}^+$ is the *a posteriori* acceleration error covariance matrix, Q_{wa} is the covariance matrix of $w_{a,t}$, and Q_{va} is the covariance of the measurement noise vector $v_{A,t}$. The last term of (24) was found by assuming that the gyroscope noise variance is equal in the x-y- and z-directions. In this case, the noise covariance matrix does not change when the noise is expressed in a different reference system.

3 Experimental methods

An inertial measurement unit (IMU) was constructed by mounting three vibrating beam gyroscopes* and three piezo-resistive accelerometers† perpendicular to each other in a $30 \times 20 \times 50$ mm³ box. These sensors were calibrated according to FERRARIS *et al.* (1995) to obtain the gains and offsets of both the accelerometers and gyroscopes.

*Murata ENC05
†AD XL05

3.1 Comparison with optokinetic system

The Kalman filter was tested by comparison of the orientation as calculated by the Kalman filter with the orientation that was obtained by a laboratory-bound 3D human motion tracking system Vicon. Three markers on 0.10 m carbon-fibre sticks, on a PVC holder, were securely attached to each sensor box to measure the sensor orientation. The accuracy of the reference measurements was estimated by looking at the relative movement between the markers. The orientation of the marker frame with respect to the IMU co-ordinate frame was obtained using the accelerometer output vector during two moments in which the IMU was put in a different orientation. Gyroscope and accelerometer signals were sampled at 100 Hz and recorded with a portable datalogger.

The IMU was placed on the pelvis, trunk and forearm. Tasks that were performed were: lifting crates, mimicking eating and mimicking typical morning routine tasks. For the crate-lifting tasks, the IMU was placed on the dorsal side of the pelvis and between the shoulder blades at the height of the T10 vertebra. The z-axis of the pelvis and trunk IMU pointed cranially, and the y-axis pointed laterally, to the left. The forearm IMU was placed on the dorsal side of the wrist, with the y-axis of the IMU unit along the arm, pointing in the proximal direction, and the z-axis pointing in the dorsal direction.

The first task was a 2 min lifting task. A stack of six empty beer crates was placed in front of the subject. The subject was asked to move the crates one by one from the stack to build a new stack 1 m away. Once the new stack was completed, the routine was reversed. This was repeated for the duration of the trial. Ten recordings were made at different lifting speeds. The pace of crate stacking was dictated by a metronome. The time intervals between the handling of two crates were 7 s, 6 s, 5 s (twice), 4 s, 3.5 s (twice), 3 s (twice) and 2 s. Two trials were performed at a pace of 3.5 s per crate, as this was experienced as a comfortable lifting speed.

The second task consisted of three trials of 90 s in which the subject was asked to mimic eating. It consisted of subsequent sessions of the following activities: pouring a glass (10 s), eating soup (20 s), eating spaghetti (20 s), eating meat (30 s), drinking (10 s). The morning-routine tasks consisted of: pouring water on face and drying it using a towel (10 s), applying deodorant (10 s), buttoning a blouse (10 s), combing hair (20 s), brushing teeth (30 s).

The tasks described were chosen, not only because of their relevance in ambulatory movement recording, but also for their very different movement characteristics and 3D character. Prior to and after each recording, the subject was asked to stand still for 4 s. The gyroscope signals that were recorded in this interval were averaged to yield the initial offset. Experiments were performed on two healthy subjects. The first subject (male, 29 years) performed the lifting task, and the second (female, 28 years) performed the eating and morning routine tasks. Both subjects signed an informed consent prior to the measurement.

3.2 Model parameter estimation

Before the Kalman filter was used, the model parameters were determined. The sensor noise variances Q_{vA} and Q_{vG} were found by taking the variance of the sensor signal while the sensor was lying still on the laboratory floor. The parameters c_a and Q_{wa} were chosen to give reasonable results while the filter was tested. Gyroscope offset variation, described by Q_{wb}, was determined with a temperature experiment.

A measurement of gyroscope and accelerometer offset fluctuation was carried out to

(i)   identify the parameter for gyroscope offset change w_b
(ii) validate the assumption that the accelerometer offset does not change because the subjects skin warms up.

It was assumed that the major factor influencing the offsets is the temperature, so that the variation due to a varying temperature is an approximation of the entire offset variation. The effect of temperature on gyroscope and accelerometer offset was measured by cooling down two IMUs in an oven from 40 to 20°C in a time period of 3 h. This was done by laying the sensor on six different sides, enabling us to measure both the gyroscope and the accelerometer offset dependence on temperature.

A practical value for gyroscope offset variation w_b could be estimated by taking the time derivative with respect to temperature at 30°C and assuming that the temperature during measurements will not fluctuate by more than $1°\,\mathrm{min}^{-1}$. A value for the change in accelerometer offset resulting from mounting an IMU on a subject was obtained using the change in output from 20 to 30°C, as this was assumed to be a typical temperature step from the calibration temperature to the temperature near the skin.

3.3 Analysis

The filter performance was split into one part describing the ability of the filter to estimate the gyroscope offset and one part describing the quality of the orientation measurement. The ability of the filter to estimate the gyroscope offset was tested by adding an error of $1\ \mathrm{rad\ s}^{-1}$ to each of the separate gyroscope channels during off-line analysis and determining the offset error at the end of each trial after applying the Kalman filter. The robustness of the filter for orientation estimation was tested by comparing the orientation errors during a trial for different tasks and one for different lifting speeds. The quality of the orientation estimation was described by the magnitude of θ_ε, expressed in the global co-ordinate system. The orientation error has different behaviour for inclination and for the orientation around the vertical. Therefore the orientation error θ_ε was split into an inclination and a heading part. When θ_ε is considered a vector, the vector component in the vertical direction is called the heading, and the component in the horizontal plane is defined as the inclination error. As long as one of these two errors is small, this is a reasonable error measure.

The heading can be interpreted as the rotation around the vertical, and the inclination error can be interpreted as the angle the estimated Z-axis makes with the real Z-axis.

The inclination of the Kalman filter was compared with the inclination obtained by low-pass filtering accelerometers. The heading error was continuously increasing, and therefore its derivative with respect to time was used to compare with the orientation that was obtained by strapdown integration of gyroscope signals. Comparisons were made with a paired t-test at a significance level of 5%.

4 Results

4.1 Accuracy of the reference measurement system

The accuracy of the reference measurements performed with the Vicon system depends on the accuracy of the position measurement of the markers and on the accuracy of the marker–sensor orientation estimate. The accuracy of the position measurement was estimated by considering the distance between two markers. The standard deviation of the fluctuation

in measured distance was 1 mm. This corresponds to a standard deviation in measured orientation of less than 1°.

Fluctuation of accelerometer offset can cause an error in sensor–marker orientation. Using the temperature experiments, the offset change of six accelerometers after a temperature step from 20 to 30° was $0.2\ \mathrm{ms}^{-2}$ on average (SD $0.2\ \mathrm{ms}^{-2}$). An offset error of $0.2\ \mathrm{ms}^{-2}$ corresponds to an angle error of 1.1°. It was assumed that these were the largest sources of error of the reference system.

4.2 Parameter identification

An example of a gyroscope and accelerometer recording is given in Fig. 4. It shows the signals of a sensor on the trunk during the lifting of one crate, involving flexion as well as lateroflexion. It can be seen that the z-component of the accelerometer output is close to $1\ g$ at the beginning and end, indicating an upright posture. As soon as the movement starts, the magnitude of the accelerometer output vector differs from $1\ g$, indicating an acceleration.

Static measurement with the sensor lying still on the laboratory floor, to obtain gyroscope and accelerometer noise, resulted in an RMS of $0.01\ \mathrm{rad\ s}^{-1}$ and $0.1\ \mathrm{m\ s}^2$, respectively. The temperature tests indicated that the temperature dependency of the gyroscope offset was $2\ \deg\ \mathrm{s}^{-1}\mathrm{°C}^{-1}$ (SD 1) for six gyroscopes. Assuming a temperature change of less than $1°\mathrm{C\ min}^{-1}$ for laboratory experiments, this corresponds to an offset change per timestep w_b of $0.3 \times 10^{-3}\ \deg\ \mathrm{s}^{-1}$. While testing the Kalman filter, it appeared that a low c_a of 0.6 and a standard deviation of each component of w_a of $0.4\ \mathrm{ms}^{-2}$ gave good results.

4.3 Orientation accuracy

An example of the filter performance during a crate-lifting trial is shown in Fig. 5. The error of the orientation obtained using the filter was compared with the integration method described by BORTZ (1971). The error was defined as the magnitude of the orientation error vector. It can be seen that the orientation error, as obtained by integration of the gyroscope signal, is larger than the error of the Kalman filter estimate. The reason that the slope of the orientation error is close to zero at the start and end of the trial is because the gyroscope offset was determined at these points.

The magnitude of the orientation drift was defined as the time derivatives of the orientation error. The heading drift
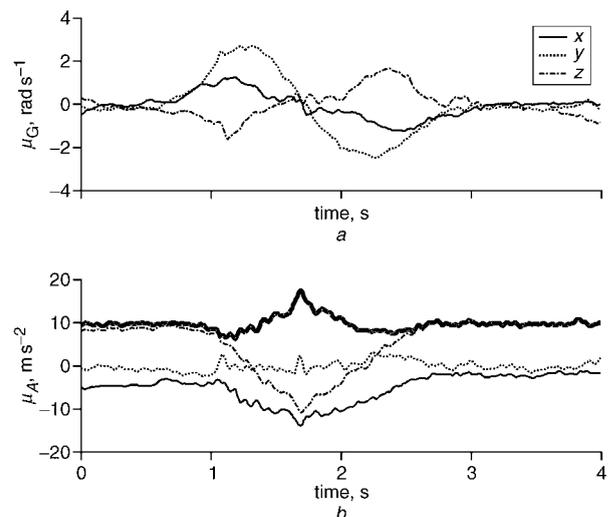

Fig. 4 *Measured sensor signals during one crate lift. Sensor is attached to trunk. (a) gyroscope output vector; (b) accelerometer output vector. Accelerometer magnitude is represented by thick line*
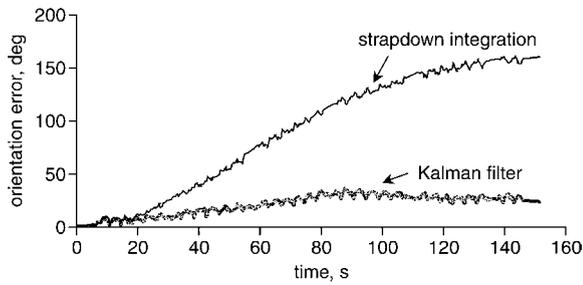
Fig. 5 *Example trial of orientation error during crate-lifting trial. Orientation error is defined as angle over which computed sensor frame has to be rotated to coincide with actual sensor frame*

was defined likewise as the time derivative of the change in heading error. The average orientation and heading drift over several trials is given in Fig. 6. Using paired *t*-tests with a 5% significance level, it was found that the orientation errors from the Kalman filter are significantly smaller than the errors obtained by integration alone. However, the heading errors from the Kalman filter are not significantly different from the heading errors from the strapdown integration algorithm.

The RMS value of the inclination error during different tasks is shown in Fig. 7. For three tasks, the inclination as computed with the Kalman filter is compared with the inclination that is obtained by low-pass filtering the accelerometer signals and applying (7). The low-pass filter is a fourth order Butterworth filter with a 5 Hz cutoff frequency. The Kalman filter performed significantly better than the method without Kalman filter. To test the robustness of the filter for the speed of movement, the influence of the lifting speed on the inclination error was determined (Fig 8). A linear regression was made between the lifting speed and inclination error. The slope was significantly different from zero and the correlation coefficient was 0.77 for the Kalman filter and 0.95 for the method using only the accelerometer. Especially at high lifting speeds, the Kalman filter shows a considerable improvement over the use of accelerometers as inclinometers.

4.4 Gyroscope offset estimation

The time required for the filter to estimate the offset was tested by off-line processing of the sensor signals using an initial offset error, artificially added to the gyroscope signals prior to application of the Kalman filter. The offset error at the end of the measurement was then used as a measure for the ability of the filter to estimate the offset.
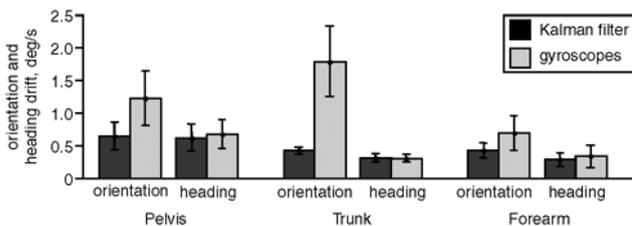

Fig. 6 *Heading and orientation drift when using Kalman filter, compared with strapdown integration of gyroscope signals only. Drift of estimated orientation during trial was obtained by taking time derivative of orientation and heading error. Inclination of pelvis and trunk were obtained during crate-lifting task (number of measurements = 10), and inclination of forearm was obtained from three morning and three eating routines*
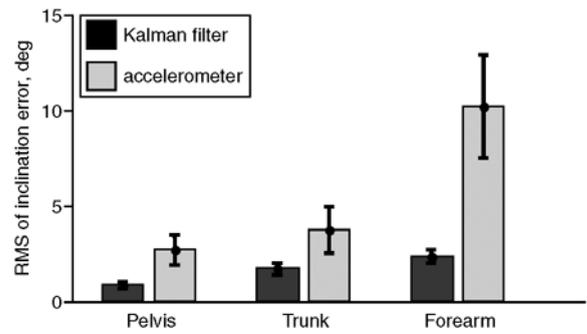

Fig. 7 *RMS value of inclination error for three types of movement, obtained using Kalman filter and using accelerometer as inclinometer. Inclination of pelvis and trunk were obtained during crate-lifting tasks (number of measurements = 10), and inclination of forearm was obtained from three morning and three eating daily routines*

An example of gyroscope offset estimation during a crate-lifting experiment is given in Fig. 9. The decline in offset that is estimated using the Kalman filter is presented using an initial offset error of 10 deg s^{-1}. Fig. 10 also gives the standard deviation estimated by the Kalman filter. These are the square roots of the three diagonal elements of $Q_{b,t}^+$. As the accelerometer gives an estimate of the inclination, merely the gyroscope offset of gyroscopes with their sensitive axes in the horizontal plane can be corrected. This is also shown in the standard deviation graph. As the *y*-axis points in the lateral direction during the entire trial, the *y*-component of the offset has the smallest covariance at the end of the trial.

The offset estimation was tested for the lifting experiments ($N = 10$), with the sensor on the trunk and pelvis, as well as for the eating and morning routine tasks together ($N = 6$), with the sensor on the forearm. The remaining offset error after 120 s is shown in Fig. 10. From the Figure, it can be seen that, for crate-lifting tasks, the estimation of the offsets in the sensor *z*-axis is most difficult. This is because the *z*-axis of the sensor co-ordinate frame is predominantly vertical during these trials.

5 Discussion

Considering Figs 6 and 7, it can be concluded that the orientation drift of the examined trials processed using the Kalman
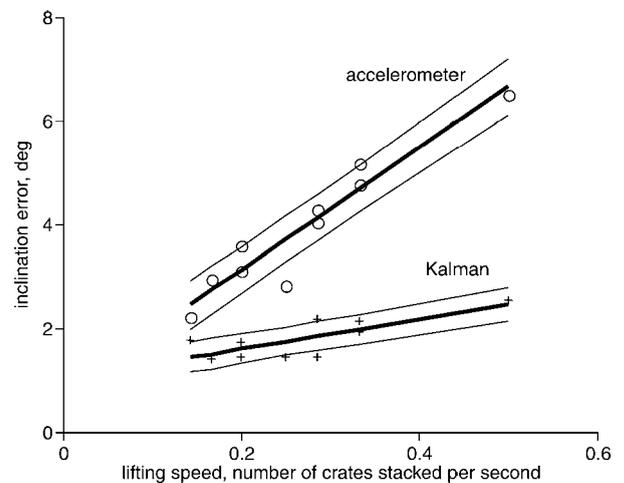

Fig. 8 *Inclination error as function of lifting speed for inclination obtained using accelerometer and Kalman filter, along with 95% confidence intervals*
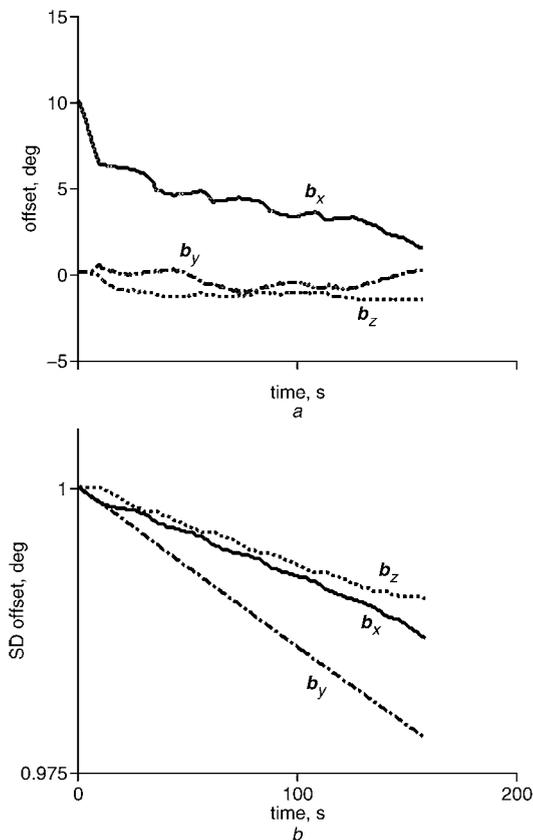
Fig. 9 *Example of offset estimation of trunk sensor during crate-lifting trial. Initial offset error was $10 \deg s^{-1}$ added to x-gyroscope. (a) Offset error; (b) offset SD, estimated by filter. Offsets of gyroscopes in horizontal plane can only be estimated on basis of inclination information from accelerometer. y-gyroscope points laterally and is, most of time, approximately in horizontal plane. Therefore offset on y-gyroscope can be estimated better than x- and z-offsets*

filter can almost completely be attributed to heading error. This is in accordance with the notion that the accelerometer signal only contains information about inclination and not about heading. In theory, the heading drift from the Kalman filter could be smaller than the heading drift of strapdown integration, because the Kalman filter estimates the offset in all three directions. However, the heading errors obtained with the Kalman filter and with the strapdown integration appeared to be almost the same. In terms of the model (Fig. 2), this would mean that the offsets are not sufficiently observable to reduce the heading drift effectively. This is in accordance with the finding that the offset estimation is especially difficult for the gyroscope that is mostly in the vertical direction (Fig. 10).
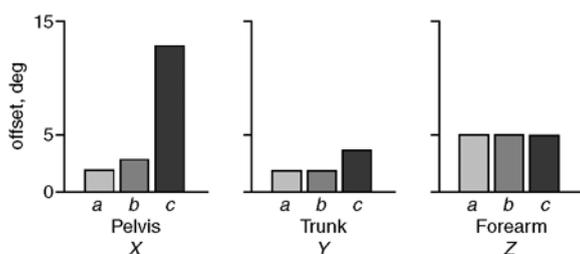

Fig. 10 *Offset estimation after trial of 120 s. Each trial was filtered using initial offset error of 1 rad applied to x-, y- and z-axes subsequently. (X) Offset error of IMU on pelvis during lifting experiment. (Y) Offset error of IMU on trunk in lifting experiment. (Z) Offset error of IMU on arm, morning routine tasks.*

For applications in which the heading is important, additional sensors or assumptions are required. For example, biomechanical constraints on the joints between segments can be used. This method could only result in an accurate orientation between two segments. Magnetic field sensors may make the heading observable (BACHMAN (2000)), but have the disadvantage that they are difficult to use in the vicinity of ferromagnetic metals.

If the inertial sensing unit is to be used during measurement of activities of daily living, the temperature may fluctuate more than in the laboratory, resulting in considerable errors because of offset fluctuation. In this case, the offset errors shown in Fig. 10 will be realistic and will give large errors in orientation estimates. The Kalman filter and sensor unit described in this article have a limited ability to track these offset changes.

The gyroscope offset estimation could be improved by use of a better spectral model for the acceleration signal. In this study, the acceleration was modelled as a low pass realisation of a white-noise signal. Therefore the Kalman filter will assume low-frequency components in the acceleration. In practice, however, a segment will never accelerate in the same direction for more than a few seconds. Therefore the acceleration will have a bandpass spectrum. If the acceleration spectrum is modelled as a bandpass spectrum, the overlap of the acceleration and gyroscope offset spectra will be less. This makes it easier for the filter to distinguish between both. A disadvantage of this method is that more assumptions restrict the general applicability of the filter.

Adding the acceleration to the state vector will not greatly improve the filter performance, whereas it will significantly increase computational burden. Because the acceleration is only moderately correlated in time, an accurate estimation of acceleration at one time step will not have a great influence on the next time step.

The experimental evaluation of the orientation estimation algorithm was conducted on two subjects, each performing part of the protocol. This does not limit generalisation, as it was not our aim to evaluate the inter-individual performance of movement tasks, but merely to evaluate the performance of the orientation estimation algorithm under the condition of representative 3D human movements. It is critical that this evaluation includes very different daily-life tasks. Therefore a lifting task, performed at different lifting speeds, and eating and morning-routine tasks were included.

Contrary to what could be expected, the orientation and heading drift of the forearm during eating and morning routine tasks was less than that of the pelvis during crate stacking, although the rotations and accelerations were larger. This could be attributed to the fact that different sensor modules were placed on different segments. As not all gyroscopes are equal, a plausible explanation would be that, coincidentally, the arm sensor performed better than the pelvis sensors.

This means that the heading drift is determined by the quality of the sensors and, to a lesser extent, by the conducted task.

The most important effect of the Kalman filter is the ability to estimate inclination. The inclination error is not only dependent on the gyroscope noise and offset but also on the acceleration. The inclination errors for different tasks (Fig. 7) give an indication of the effect of the Kalman filter. These errors are within the specifications required by most applications.

Because of the heading drift, the proposed Kalman filter will only be useful for long measurements if only an accurate inclination is required. There are, however, many applications that require only short measurements or for which the heading is not important. A Kalman filter for estimating inclination merely using accelerometers was described in LUINGE and VELTINK (2004). For measuring trunk and pelvis inclination

during lifting tasks, the RMS value of the inclination error obtained using the Kalman filter for accelerometer signals only was in the same order as when using accelerometers and gyroscopes. This means that, for these tasks, the relatively heavy and power-consuming gyroscopes could be omitted. The advantage of applying gyroscopes, however, is that angular velocity and a short-term estimate of total orientation are available.

References

ALUSI, S. H., WORTHINGTON, J., GLICKMAN, S., and BAIN, P. G. (2001): 'A study of tremor in multiple sclerosis', *Brain: J. Neurol.*, **124**, pp. 720–730

BACHMAN, E. R. (2000): 'Inertial and magnetic tracking of limb segment orientation for inserting humans in synthetic environments'. Naval postgraduate school, Monterey, USA.

BARSHAN, B., and DURRANT-WHYTE, H. F. (1995): 'Inertial navigation systems for mobile robots', *IEEE Trans. Robot. Automat.*, **11**, pp. 328–342

BASELLI, G., LEGNANI, G., FRANCO, P., BROGNOLI, F., MARRAS, A., QUARANTA, F., and ZAPPA, B. (2001): 'Assessment of inertial and gravitational inputs to the vestibular system', *J. Biomech.*, **34**, pp. 821–826

BATEN, C. T. M., OOSTERHOFF, P., KINGMA, I., VELTINK, P. H., and HERMENS, H. J. (1996): 'Inertial sensing in ambulatory load estimation'. *Proc. IEEE Eng. in Med. & Biol Soc., 18th Ann. Int. Conf.*, Amsterdam

BERNMARK, E., and WIKTORIN, C. (2002): 'A triaxial accelerometer for measuring arm movements', *Appl. Ergon.*, **33**, pp. 541–547

BORTZ, J. E. (1971): 'A new mathematical formulation for strapdown inertial navigation', *IEEE Trans. Aerosp. Electron. Syst.*, **7**, pp. 61–66

BOUTEN, C. V. C., KOEKKOEK, K.T.M., VERDUIN, M., KODDE, R., and JANSSEN, J.D. (1997): 'A triaxial accelerometer and portable processing unit for the assessment of daily physical activity', *IEEE Trans. Biomed. Eng.*, **44**, pp. 136–147

BROWN, R. G., and HWANG, P. Y. C. (1997): '*Introduction to random signals and applied Kalman filtering*' (John Wiley and Sons, 1997)

DINGWELL, J. B., CUSUMANO, J. P., STERNAD, D., and CAVANAGH, P. R. (2000): 'Slower speeds in patients with diabetic neuropathy lead to improved local dynamic stability of continuous overground walking', *J. Biomech.*, **33**, pp. 1269–1277

FERRARIS, F., GRIMALDI, U., and PARVIS, M. (1995): 'Procedure for effortless in-field calibration of three-axis rate gyros and accelerometers', *Sensors Mater.*, **7**, pp. 311–330

FOERSTER, F., SMEJA, M., and FAHRENBERG, J. U. (1999): 'Detection of posture and motion by accelerometry: a validation study in ambulatory monitoring', *Comput. Human Behav.*, **15**, pp. 571–583

FOXLIN, E. (1996): 'Inertial head-tracker sensor fusion by a complementary separate -bias Kalman filter'. *Proc. VRAIS*

HANSSON, G. A., ASTERLAND, P., HOLMER, N. G., and SKERFVING, S. (2001): 'Validity and reliability of triaxial accelerometers for inclinometry in posture analysis', *Med. Biol. Eng. Comput.*, **39**, pp. 405–413

IGNAGNI, M. B. (1990): 'Optimal strapdown attitude integration algorithms', *J. Guidance*, **12**, pp. 363–369

JIANG, Y. F., and LIN, Y. P. (1992): 'Improved strapdown coning algorithms', *IEEE Trans. Aerosp. Elec. Syst.*, **28**, pp. 484–489

KALMAN, R. E. (1960): 'A new approach to linear filtering and prediction problems', *J. Basic Eng.*, pp. 35–45

KEMP, B., JANSSEN, A. J. M. W., and VAN DER KAMP, B. (1998): 'Body position can be monitored in 3D using miniature accelerometers and earth-magnetic field sensors', *Electroenceph. Clin. Neurophysiol./Electromyogr. Motor Control*, **109**, pp. 484–488

LÖTTERS, J., BOMER, J., VERLOOP, T., DROOG, E., OLTHUIS, W., VELTINK, P. H., and BERGVELD, P. (1998): 'In-use calibration procedure for a triaxial accelerometer', *Sensors Actuators A, Phys.*, **66**, pp. 205–212

LUINGE, H. J., and VELTINK, P. H. (2004): 'Inclination measurement of human movement using a 3D accelerometer with autocalibration', *IEEE Trans. Neural Syst. Rehabil. Eng.*, **12**, pp. 112–121

MANSON, A. J., BROWN, P., O'SULLIVAN, J. D., ASSELMAN, P., BUCKWELL, D., and LEES, A. J. (2000): 'An ambulatory dyskinesia monitor', *J. Neurol. Neurosurg. Psychiatry*, **68**, pp. 196–201

MATHIE, M. J., COSTER, A. C., LOVELL, N. H., and CELLER, B. G. (2003): 'Detection of daily physical activities using a triaxial accelerometer', *Med. Biol. Eng. Comput.*, **41**, pp. 296–301

MAYAGOITIA, R. E., NENE, A. V., and VELTINK, P. H. (2002): 'Accelerometer and rate gyroscope measurement of kinematics: an inexpensive alternative to optical motion analysis systems', *J. Biomech.*, **35**, pp. 537–542

MIYAZAKI, S. (1997): 'Long-term unrestrained measurement of stride length and walking velocity utilizing a piezoelectric gyroscope', *IEEE Trans. Biomed. Eng.*, **44**, pp. 753–759

MOE-NILSSEN, R. (1998): 'A new method for evaluating motor control in gait under real-life environmental conditions. Part 1: The instrument', *Clin. Biomech.*, **13**, pp. 328–335

MOE-NILSSEN, R., and HELBOSTAD, J. L. (2004): 'Trunk accelerometry as a measure of balance control during quiet standing', *J. Biomech.*, **37**, pp, 121–126

NAJAFI, B., AMINIAN, K., LOEW, F., BLANC, Y., and ROBERT, P. A. (2002): 'Measurement of stand-sit and sit-stand transitions using a miniature gyroscope and its application in fall risk evaluation in the elderly', *IEEE Trans. Biomed. Eng.*, **49**, pp. 843–851

PAPPAS, I. P., POPOVIC, M. R., KELLER, T., DIETZ, V., and MORARI, M. (2001): 'A reliable gait phase detection system', *IEEE Trans. Neural Syst. Rehabil. Eng.*, **9**, pp. 113–125

SWEENEY, P. C., LYONS, G. M., and VELTINK, P. H. (2000): 'Finite state control of functional electrical stimulation for the rehabilitation of gait', *Med. Biol. Eng. Comput.*, **38**, pp. 121–126

TONG, K. Y., and GRANAT, M. H. (1998): 'Virtual artificial sensor technique for functional electrical stimulation', *Med. Eng. Phys.*, **20**, pp. 458–468

TONG, K., and GRANAT, M. H. (1999): 'A practical gait analysis system using gyroscopes', *Med. Eng. Phys.*, **21**, pp. 87–94

USWATTE, G. (2000): 'Objective measurement of functional upper-extremity movement using accelerometer recordings transformed with a threshold filter', *Stroke*, **31**, pp. 662–667

VAN DEN BOGERT, A. J., READ, L., and NIGG, B. M. (1996): 'A method for inverse dynamic analysis using accelerometry', *J. Biomech.*, **29**, pp. 949–954

VELTINK, P. H., SLYCKE, P., HEMSSEMS, J., BUSCHMAN, R., BULTSTRA, G., and HERMENS, H. (2003): 'Three dimensional inertial sensing of foot movements for automatic tuning of a two-channel implantable drop-foot stimulator', *Med. Eng. Phys.*, **25**, pp. 21–28

WILLEMSEN, A. T., BLOEMHOF, F., and BOOM, H. B. (1990a): 'Automatic stance-swing phase detection from accelerometer data for peroneal nerve stimulation', *IEEE Trans. Biomed. Eng.*, **37**, pp. 1201–1208

WILLEMSEN, A. T., VAN ALSTE, J. A., and BOOM, H. B. (1990b): 'Real-time gait assessment utilizing a new way of accelerometry', *J. Biomech.*, **23**, pp. 859–863

WILLIAMSON, R., and ANDREWS, B. J. (2000): 'Sensor systems for lower limb functional electrical stimulation (FES) control', *Med. Eng. Phys.*, **22**, pp. 313–325

WILLIAMSON, R., and ANDREWS, B. J. (2001): 'Detecting absolute human knee angle and angular velocity using accelerometers and rate gyroscopes', *Med. Biol. Eng. Comput.*, **39**, pp. 294–302

Authors' biographies

HENK J. LUINGE studied Mechanical Engineering at the University of Twente (M.Sc. 1998) and performed PhD research on the topic of inertial sensing of human movement (PhD 2002). After working at Xsens technologies he began a postdoctoral fellowship at the Sensory Motor Performance Program at the Rehabilitation institute of Chicago. He is currently working on a system for capturing the movements and forces of a horses hoof at the Ecole Nationale Vétérinaire d'Alfort.

PETER H. VELTINK studied Electrical Engineering at the University of Twente (M.Sc. 1984) where he also performed his PhD research

in the area of electrical nerve stimulation (PhD 1988). Currently, he is a professor of technology for the restoration of human function at the University of Twente, Institute for Biomedical Technology (BMTI), and performs research in the area of artificial motor control and ambulatory sensory systems with applications to rehabilitation medicine. He is the scientific coordinator of the EU training networks NeuralPRO (2000-2004) and NEUROS (1996-2000). He has been the UT project leader in several European projects (BIOMED2 Sensations project, CREST project, Concerted Actions RAFT). He performed sabbaticals at Case Western Reserve University, Cleveland, in 1989 and at the Center for Sensory-Motor-Interaction at Aalborg University in 1997. He has been the treasurer of the International Functional Electrical Stimulation Society (IFESS) from 1996 to 2001. Prof. Veltink received the Royal Shell Stimulating Prize for his contribution to the rehabilitation-engineering field in 1997.